Acc. Chem. Res. **2002,** *35,* 366−375

Computational Studies of the Gramicidin Channel

BENOÎT ROUX*

Department of Biochemistry, Weill Medical College of Cornell University, 1300 York Avenue, New York, New York 10021

Received September 17, 2001

ABSTRACT

Ion channels are highly specific membrane-spanning protein structures which serve to facilitate the passage of selected ions across the lipid barrier. In the past decade, molecular dynamics simulations based on atomic models and realistic microscopic interactions with explicit solvent and membrane lipids have been used to gain insight into the function of these complex systems. These calculations have considerably expanded our view of ion permeation at the microscopic level. This Account will mainly focus on computational studies of the gramicidin A channel, one of the simplest and best characterized molecular pore.

I. Introduction

The gramicidin A (GA) channel is currently the best characterized molecular pore, structurally and functionally.[1−3] In a phospholipid bilayer membrane, this small pentadecapeptide adopts a head-to-head β-helical dimer conformation to form an ion-conducting narrow pore of about 4 Å in diameter.[4−7] The three-dimensional structure is illustrated in Figure 1. The hydrogen-bonded carbonyls line the pore, and the alternating D- and L-amino acid side chains, most of them hydrophobic, extend away into the membrane lipid. The diameter of the pore is such that the permeation process involves the translocation in single file of the ion and water molecules through the channel interior, the large energetic loss due to dehydration being compensated by coordination with the backbone carbonyl oxygens.

The GA channel appears to be ideally selective for small univalent cations, as it is blocked by divalent cations and completely impermeable to anions.[2] Chemically modified GA channels can be directly synthesized, the number of possible chemical variations being virtually unlimited. GA and its related variants exhibit functional behavior similar to far more complex macromolecular biological structures and for this reason have proved to be extremely useful model systems to study the principles governing ion transport across lipid membranes.

Molecular dynamics (MD) simulations can contribute greatly to our understanding of ion channels. The first MD simulations of an ion channel based on a fully flexible atomic model were carried out by Mackay, Berens, Wilson, and Hagler[8] nearly 20 years ago, shortly after the early development in protein simulations.[9] Those calculations, which included only the GA channel, one cation, and 13 water molecules, had a lasting impact on all subsequent computational studies of ion channels (for a review, see ref 3). The significant increase in computational power, and the developments in computational methodologies of the past decade, have made it possible to extend the approach considerably. Although this Account is focused on simulations of the GA channel, our aim is to provide a general overview of the computational methods used in MD studies of ion channels.

II. Methodologies

(a) Microscopic Potential Function. For meaningful theoretical studies of permeation, it is necessary to have a potential energy function providing a realistic and accurate representation of the microscopic interactions. This presents a difficult challenge: the conductance of the GA channel results from a delicate balance of very strong microscopic interactions, the large energetic loss of dehydration being roughly compensated by coordination with main-chain carbonyl oxygens. Gas-phase experiments[10,11] and ab initio calculations[12] on model systems provide the most direct information concerning the individual microscopic interactions. The interactions of ions with a single water molecule or with a single isolated *N*-methylacetamide (NMA) molecule, an excellent model of the backbone carbonyl of proteins, are of particular interest. Solvation free energies of cations in liquid water and liquid NMA are also very important for calibrating the potential function. In the case of water, it is possible to reproduce both the microscopic interactions and the solvation free energy of ions with the current potential functions.[13,14] In contrast, MD free energy calculations indicate that it is very difficult to reproduce both the cation−NMA microscopic energy and the solvation free energy in liquid NMA with current biomolecular potential functions. Additional problems arise from the uncertainty in the experimental values of the free energy of solvation of small ions.[15]

Current biomolecular potential functions try to account for many-body polarization effects in an average way using an effective parametrization of the atomic partial charges. Because of this approximation, the optimal parametrization is the result of a compromise between an accurate representation of the microscopic energies and bulk solvation properties. In principle, it is possible to reproduce both microscopic energies and thermodynamic free

Benoît Roux was born in Montreal in 1958. He first studied in the Physics Department at the Université de Montréal, where he received a B.S. in 1981 and a M.S in 1984. He then pursued his graduate studies at Harvard, where he received a Ph.D. in biophysics in 1990 under the supervision of Martin Karplus. After a year of postdoctoral research as the Commissariat à l'Energie Atomique (CEA) in Paris, he accepted a joint faculty position in the Physics and Chemistry Departments at the Université de Montréal in 1992. Over the past decade, his work has been mostly focussed on the investigation of the function of ion channels and the development of statistical mechanical methods for computing the solvation free energy of biological molecules. In 1998, he was awarded the Rutherford Medal from The Royal Society of Canada for his work. Since 1999, he has been Professor in the Department of Biochemistry at the Weill Medical College of Cornell University.

* Tel.: (212) 746-6018. Fax: (212) 746-4843. E-mail: benoit.roux@med.cornell.edu.

10.1021/ar010028v CCC: $22.00
Published on Web 03/15/2002

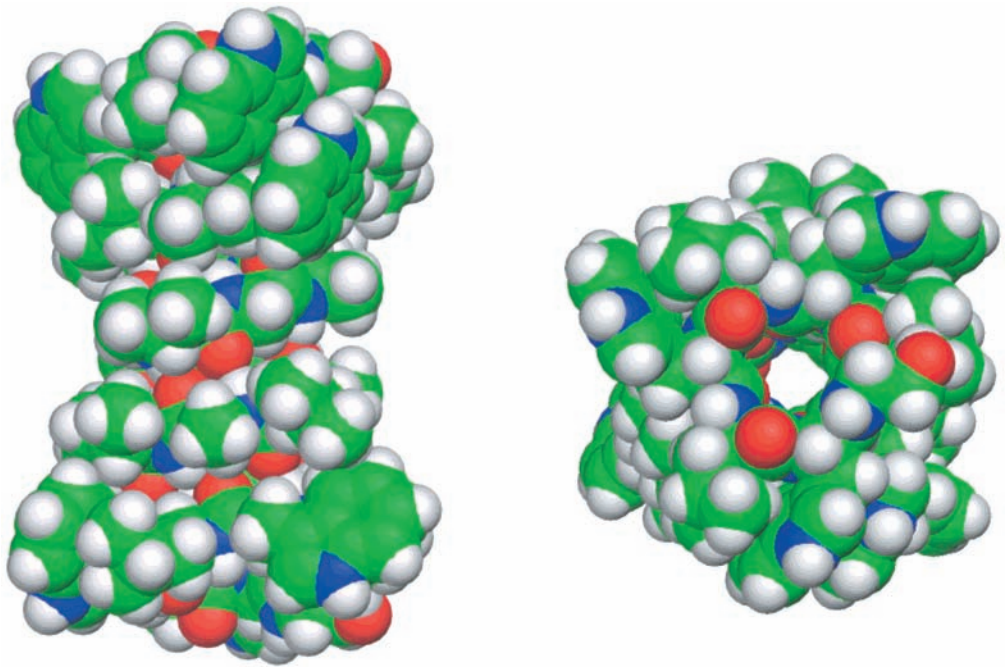

FIGURE 1. Gramicidin A (GA) channel in the head-to-head β-helix dimer conformation determined by solid-state NMR.[5,6]

energy accurately if nonadditive induced polarization effects are incorporated. A number of studies of GA have incorporated induced polarization based on some approximations,[16−18] but no general treatment is yet available.

(b) Simulation Techniques. Theoretical studies of ion channels present a number of specific difficulties due to the nature and the time scale of the microscopic processes under consideration. In particular, while typical MD trajectories are limited to several nanoseconds, the translocation of a single ion across a membrane could take on the order of a microsecond, and gating transitions are often on the order of several milliseconds.[1] For this reason, a number of computational approaches that go beyond simple "brute force" MD simulations have become essential tools in theoretical studies of ion channels.

In particular, the perturbation technique[19] or the "umbrella sampling" procedure[20] can be used to calculate the potential of mean force (PMF) of ions along the channel axis;[18,21] the reactive flux algorithm[22] and the generalized Langevin equation[23] can be used to calculate the transition rate of gating transitions and activated processes occurring on very long time scales;[24] alchemical MD free energy simulations (MD/FES) such as thermodynamic integration (TI) or free energy perturbation (FEP) techniques[25] can be used to calculate relative solvation free energies of ions in the channel;[17,26] discretized Feynmann path integral representation of the density matrix[27] can be used to incorporate quantum mechanical effects in proton exchange processes;[28] continuum dielectric methods based on the Poisson−Boltzmann (PB) equation can be used to estimate long-range electrostatic effects.[29−31]

(c) Construction of a Starting Configuration. The wide range of sophisticated computational techniques listed in section II.b can be performed using a biomolecular simulation program such as CHARMM.[32] This is indicative of the fact that MD simulations of biomolecular systems can be applied almost routinely today. There are, however, important additional problems in simulating protein−membrane complexes that must be addressed specifically. In particular, the construction of a reasonable starting configuration to simulate a protein in a fully solvated explicit phospholipid bilayer is challenging. Because of the very slow configurational relaxation present in the membrane environment (see Chapter 1 in ref 33), current trajectories which are typically on the order of a few nanoseconds can mostly explore the neighborhood of a starting configuration. To reduce the computer time needed for equilibration, a procedure was developed for assembling protein−membrane complexes from pre-equilibrated and pre-hydrated phospholipid molecules in configurations that correspond as closely as possible to the equilibrated state of the system.[34,35] The method is an extension of the approach used by Pastor and co-workers to generate pure lipid bilayers.[36] To construct the configuration, lipid molecules taken in random conformers analogous to those found in a fluid bilayer are disposed around the protein as elementary building blocks. The initial configuration is then refined and equilibrated until no systematic changes are observed. The membrane construction method was used to generate initial configurations for the GA channel embedded in a fully hydrated dimyristoyl phosphatidycholine (DMPC) bilayer.[34,35]

(d) Solid-State NMR. Measurements from solid-state nuclear magnetic resonance (NMR) provide particularly valuable information about membrane−protein systems. In particular, the three-dimensional structure of GA in a DMPC bilayer was determined using solid-state NMR measurements such as deuterium quadrupolar splittings, dipolar couplings, chemical shifts, and chemical shift anisotropy.[5] The structure was refined using the NMR measurements as energy restraints.[6] Such an approach

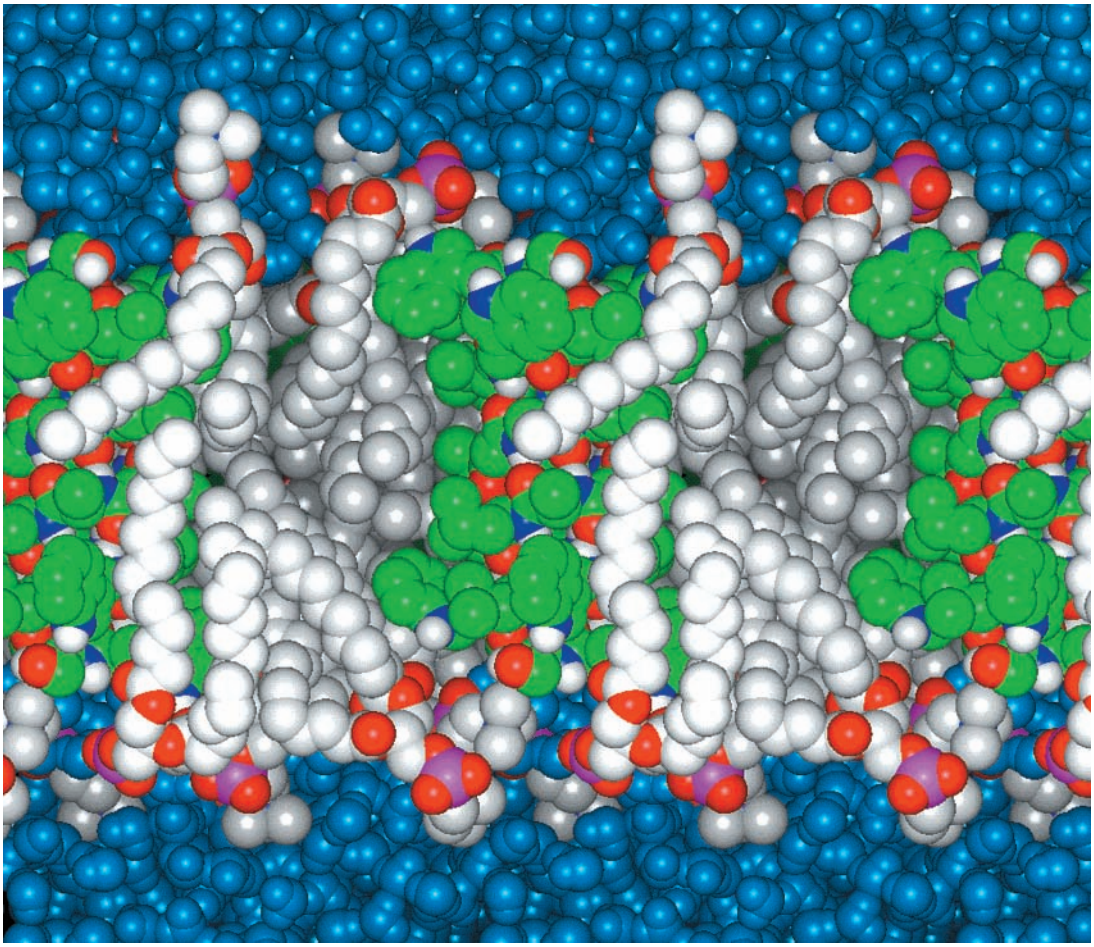

FIGURE 2. Molecular graphics representation of the GA:DMPC system[35] (it should be noted that the neighboring images from the periodic boundary conditions are seen in the figure).

relies on important assumptions. First, it is assumed that the shielding tensor orientation is fixed relative to the local molecular frame and that the magnitude of the components is constant. In addition, it is assumed that a single average molecular conformation is representative of the three-dimensional channel structure. In fact, further analysis based on ab initio density functional calculations revealed that these assumptions are not perfectly satisfied.[37] Furthermore, observed properties result from a time average over rapidly fluctuating quantities because the time scale of solid-state NMR is much slower than that of rapid molecular motions. This implies that a time average over instantaneous values along the trajectory must be performed to calculate observed properties.

III. Results

(a) Membrane Environment. The GA channel is strongly affected by its environment.[2] In particular, it can adopt the β-helical ion-conducting conformation only when it is embedded in detergent micelles[4,7] or in a phospholipid bilayer.[5] To better characterize the environment provided by the lipid bilayer, the GA channel was simulated in a fully hydrated DMPC bilayer.[34,35] The simulated systems, constructed with a GA:DMPC ratio of 1:8 and 45% weight water, were models of the oriented samples utilized in solid-state NMR experiments.[5] A typical configuration of the system is shown in Figure 2.

Analysis of the simulation revealed that the dynamical aspects of the protein−membrane complex are important. In particular, the membrane−solution interface region is much broader than pictured traditionally. The headgroup and glycerol regions span a region of 15 Å in width, and the water density decreases smoothly throughout the polar head region, reaching the edge of the hydrocarbon chains region and the carbonyl oxygens of the ester group of the lipids. In Figure 3, a superposition of five configurations of the GA channel taken at a time interval of 50 ps along the trajectory is shown. It is observed that the channel undergoes significant structural fluctuations around an average conformation. The root-mean-square (rms) fluctuations of the channel are significant, on the order of 1.5 Å for the backbone atoms. The nonpolar Val and Leu side chains, pointing into the lipid hydrocarbon, are able to isomerize between various conformers on a nanosecond time scale. In contrast, the Trp side chains fluctuate around a dominant conformation, the polar N−H group of the Trp indole side chains remaining close to the membrane−solution interface. Hydrogen bonds between the Trp indole ring and the ester carbonyl group of the glycerol backbone of the DMPC were observed. Functional studies have demonstrated that the interaction

FIGURE 3. Superposition of five configurations of the GA channel separated by 50 ps taken along the MD trajectory.[34]

of the Trp with the bilayer environment is an important factor in the stability of the GA dimer in a membrane;[38] substitutions of the Trp by Phe have an important influence on the conductivity and on the average lifetime of the channel. More generally, the presence of an aromatic residue (Trp, Tyr, and Phe) at the membrane−solution interface appears to be a recurrent feature of membrane−protein (see ref 39 and references therein). Calculated time-averaged solid-state NMR properties such as ^{15}N chemical shift and ^{1}H−^{15}N dipolar coupling have been shown to be in excellent agreement with experimental data, indicating that the trajectory is sampling a meaningful ensemble of configurations.[34]

The GA:DMPC simulations clarified conflicting interpretations of the lipid acyl chain order parameters extracted from deuterium quadrupolar splittings.[40] Rice and Oldfield suggested that the irregular surface of the GA induces a disorder along the lipid acyl chains in direct contact with the channel, whereas the boundary lipids surrounding the GA present a smoother surface which, in turn, orders the next layer of lipids.[40] According to this interpretation, the observed variations in lipid order as a function of GA concentration result from the change in the population of boundary lipids versus free lipids. In contradiction with this assumption, the results from the GA:DMPC simulations showed that there is an ordering of the lipid chains in direct contact with the GA channel.[35] This ordering has also been observed in other simulations of the GA channel.[41,42]

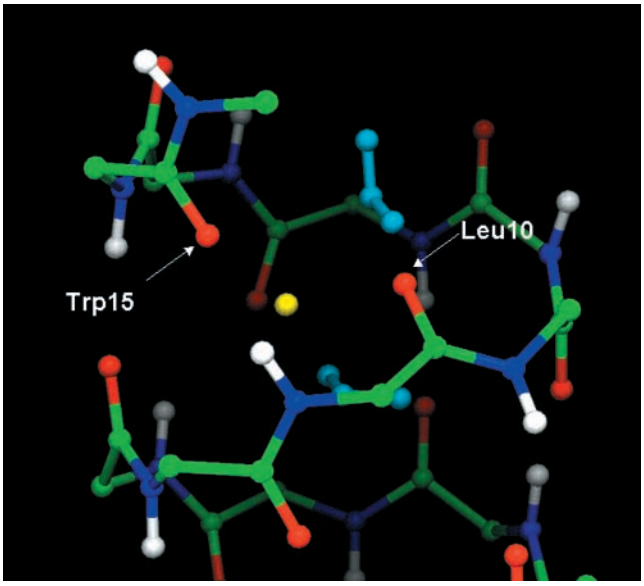

FIGURE 4. Side view of Na^+ ion in the binding site near the channel entrance determined from the analysis of solid-state NMR data.[18] For clarity, only the backbone atoms and the two nearest single-file waters are represented.

(b) Binding Site of Na^+. Detailed information about energetically favorable binding sites along the pathway of a permeating ion is essential to understand the function of a transmembrane ion channel at the molecular level. In the absence of a high-resolution structure from X-ray crystallography, measurements from solid-state NMR experiments provide the most direct information on the detailed structure of the cation binding site in the GA channel. The measurements determined the change, due to the presence of Na^+, in the ^{13}C and ^{15}N chemical shift anisotropy at specific GA backbone sites.[43,44] However, a direct structural interpretation of the NMR data is not straightforward. The observed data result from an average over rapidly fluctuating cation positions in fast exchange on the time scale of NMR. For a meaningful analysis, it is necessary to consider a dynamical average of the NMR observables over a large number of configurations.[18]

To help interpret the solid-state NMR data, a series of MD simulations with a Na^+ constrained at different positions along the channel axis were generated.[18] Combining all the information from the simulations showed variations in the NMR observables as the ion moves along the GA channel axis. To reproduce the experimental observations, these position-dependent averages must be be integrated with respect to the probability distribution of the ion along the channel axis. A semiempirical approach combining the information from both the simulations and the ^{13}C experiments was used to find the most plausible location of the main Na^+ binding site. The position of the binding site was deduced by empirically matching the magnitude of the observed chemical shift anisotropy of ^{13}C-labeled GA. The accord was found when the ion was centered at 9.2 Å from the center of the channel. The ion in its binding site is shown in Figure 4.

Comparison with the structure of the unoccupied channel showed that there were no large distortions of

the channel due to the presence of the ion. In the binding site the Na^+ is lying slightly off axis, making contacts with the carbonyl oxygen of Leu10, Trp15, and two single-file water molecules. The main channel ligand is provided by the carbonyl group of the Leu10−Trp11 peptide linkage, which exhibits the largest deflection from the ion-free channel structure (on the order of 10−15°). Interestingly, in the β-helical structure, Leu10 corresponds to the first backbone carbonyl oxygen pointing toward the bulk solvent which is not forming a hydrogen bond with a backbone amide. For this reason, it is able to provide a ligand for a cation without the energetic cost of losing a backbone hydrogen bond.

The position of the binding site determined from the analysis is remarkably consistent with previous estimates. In particular, the lowest minimum in the free energy profile of Na^+ along the axis of the GA channel calculated with MD and the perturbation technique was found at 9.2 Å.[21] In addition, analysis of ion-flux data indicated that the cation in the binding site is 14% into the transmembrane potential, which corresponds to about 9 Å using the constant field assumption[2] (but see also the next section). Last, low-angle X-ray scattering on GA incorporated in oriented dilauroylphosphatidylcholine bilayers showed that there is a binding site for Tl^+ at 9.6 ± 0.3 Å from the center of the dimer channel.[45]

(c) Transmembrane Potential. The transmembrane potential acts as a driving force on permeating ions. At the microscopic level it arises from a small charge imbalance distributed in the neighborhood of the membrane−solution interface.[29] MD simulations of a realistic representation of the membrane potential at physiological concentration, however, would require a prohibitively large atomic system and are currently impractical. To formulate a suitable approximation based on continuum electrostatics, it is useful to separate the microscopic channel system into a pore region containing n ions at fixed positions $\mathbf{r}_i$, and two bulk regions, I and II. The ionic solution on side I of the bulk region is in equilibrium with an electrode at zero potential, and the solution on side II of the bulk region is in equilibrium with an electrode at potential V_{mp}. While all the ions in the pore region are represented explicitly, it is assumed that the ions in the bulk regions I and II are represented implicitly. Based on this construct, the total free energy can be written in the form[30]

$$\Delta G_{tot} = \Delta G_0(\mathbf{r}_1, \mathbf{r}_2, ...) + \sum_i q_i \phi_{mp}(\mathbf{r}_i) + ... \qquad (1)$$

where ΔG_0 is the intrinsic free energy in the absence of any transmembrane potential, and $\phi_{mp}(\mathbf{r})$ is the contribution from the potential difference across the membrane. $\phi_{mp}(\mathbf{r})$ is calculated from the modified PB equation[29,30]

$$\nabla\cdot[\epsilon(\mathbf{r})\nabla\phi_{mp}(\mathbf{r})] = 0, \qquad \text{pore region}$$

$$\nabla\cdot[\epsilon(\mathbf{r})\nabla\phi_{mp}(\mathbf{r})] - \bar{\kappa}^2(\mathbf{r})[\phi_{mp}(\mathbf{r})] = 0, \text{ bulk region, side I}$$

$$\nabla\cdot[\epsilon(\mathbf{r})\nabla\phi_{mp}(\mathbf{r})] - \bar{\kappa}^2(\mathbf{r})[\phi_{mp}(\mathbf{r}) - V_{mp}] = 0, \qquad \text{bulk region, side II}$$

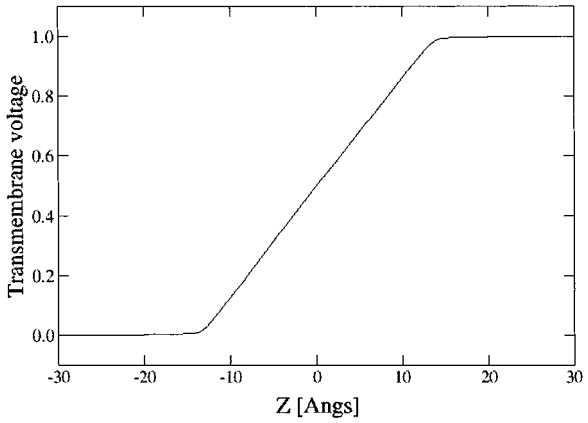

FIGURE 5. Transmembrane field ϕ_{mp} along the GA channel axis calculated by solving eq 2 numerically.[30]

where $\epsilon(\mathbf{r})$ and $\bar{\kappa}(\mathbf{r})$ are the space-dependent dielectric constant and Debye−Hückel screening factor, and V_{mp} is the equilibrium electrode potential far away on side II. When $V_{mp} = 0$, the modified PB eq 2 is reduced to the standard PB equation.

The transmembrane potential along the GA channel was calculated by solving eq 2 with a finite-difference method implemented in the PBEQ module[46] of CHARMM.[32] In the calculation, the channel and the membrane were represented in full atomic detail, while the solution was represented as a uniform dielectric constant of 80 with a salt concentration of 150 mM. The calculated transmembrane potential field along the channel axis is shown in Figure 5. The field is clearly linear, though there are small deviations near the entrance of the channel. The cation binding site, around 9 Å at the entrance of the channel, is roughly at 10−20% of the transmembrane potential, in excellent agreement with ion-flux measurements[2] (see also section III.b above).

(d) Valence Selectivity. The GA channel is ideally selective for cations while it is virtually impermeable to anions.[2] Such valence specificity is one of the simplest forms of ion selectivity. Interestingly, no obvious mechanism for charge discrimination is suggested on the basis of the three-dimensional structure of the channel because it carries no net charge and all its side chains are nonpolar. To examine the valence specificity of GA, the free energy difference of K^+ and Cl^- for the interior of the channel was calculated using MD/FES.[26] K^+ and Cl^- were chosen for the sake of simplicity because their solvation free energies are both on the order of −80 kcal/mol in liquid water. The result of the calculation showed that the environment of the pore interior is particularly unfavorable for anions relative to cations. The relative free energy, $G_{Cl}(GA) - G_{Cl}(water) - G_K(GA) + G_K(water)$, obtained from MD/FES calculations is on the order of almost +60 kcal/mol.[26] Thus, Cl^- has a much lower affinity for the interior of the channel than K^+, even though they have the same solvation free energy in bulk water.

The large free energy difference could be understood by considering the radial distribution around the ions. In bulk water, the K^+ ion is surrounded by approximately 7.4 water molecules in the first solvation shell. The oxygen

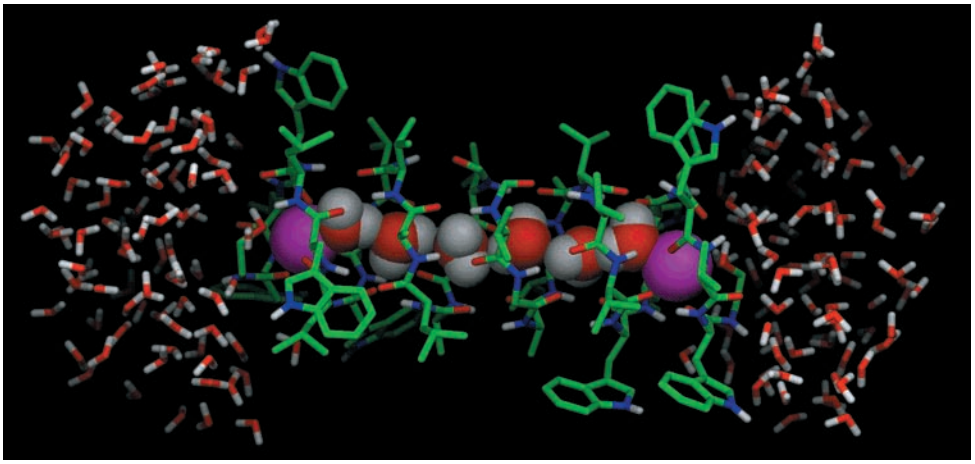

FIGURE 6. Configuration of the GA channel occupied by two Na^+ ions used in the MD/FES calculations.[17]

of the water molecules provides the favorable electrostatic interaction energy in solution. In the channel, the solvation is provided primarily by the oxygen of the backbone carbonyl group. Although the two environments are significantly different, the resulting radial distributions around K^+ are very similar. In contrast, the radial distributions around a Cl^- in bulk water and in the channel are markedly different. In bulk solution, the water molecules provide a favorable electrostatic interaction energy by forming hydrogen bonds with the anion, whereas similar hydrogen bonds with the NH amide backbone group are not easily formed in the channel. Thus, although the channel is electrically neutral, the strong asymmetry in the permanent charge distribution of the peptide backbone results in a significant reduction of favorable interaction energy in the channel for negatively charged ions.

(e) Multiple Occupancy. At moderately high concentration, the GA channel can be occupied simultaneously by two ions (see ref 17 for a review). Remarkably, double occupancy appears to be species-dependent. Analysis of ion-flux experiments indicates that, although double occupancy of the GA channel is less favorable than single occupancy for all cations, it is relatively more favorable for the large cations (K^+, Rb^+, and Cs^+) than for the small ones (Li^+ and Na^+). This can be expressed as $\Delta\Delta G^{SD}(Li) \gg \Delta\Delta G^{SD}(Na) > \Delta\Delta G^{SD}(K) \approx \Delta\Delta G^{SD}(Rb) \approx \Delta\Delta G^{SD}(Cs)$, with

$$\Delta\Delta G^{SD} = \Delta G^{D} - \Delta G^{S} \qquad (3)$$

where ΔG^S and ΔG^D are the binding free energy of a first ion to an unoccupied channel and the binding free energy of a second ion to a singly occupied channel, respectively.

The relative single-to-double occupancy free energy was calculated using MD/FES for the five cations Li^+, Na^+, K^+, Rb^+, and Cs^+.[17] The results are given in Table 1. The microscopic model of the GA channel occupied with two Na^+ used in the calculations is shown in Figure 6; six water molecules separate the ions in the doubly occupied state. The results are given in Table 1. They reveal, in agreement with experimental observations, that the doubly occupied state is relatively more favorable for the larger ions. According to MD/FES, the repulsion between two Na^+ ions occupying the binding sites in the GA channel is about 1.4 kcal/mol larger than the corresponding repulsion between two K^+. The calculations showed that ion−ion interactions are affected, in a nontrivial way, by the environment of a narrow molecular pore. In the doubly occupied state the two cation are separated by almost 20 Å (see section III.b above). In liquid water, the ion−ion interaction would be well approximated by a shielded Coulomb law, $q^2/\epsilon_w r$ (independent of the ionic radius), at such a distance. A decomposition of the free energy, given in Table 1, indicated that the difference in free energy arises mostly from the properties of the six water molecules disposed in single file inside the narrow channel. Small cations such as Li^+ or Na^+ are relatively better solvated in the singly occupied state than in the doubly occupied state, while bigger cations such as K^+, Rb^+, or Cs^+ are almost as well solvated in both the singly and doubly occupied states.

Table 1. Relative Free Energy of Double Occupancy in the GA Channel (kcal/mol)[a]

ion	total free energy	contribution from single-file water	contribution from carbonyl oxygens
Li^+	3.6	5.9	−3.2
Na^+	1.2	4.0	−3.1
K^+	−0.2	1.0	−1.8
Rb^+	0.3	0.3	−0.7
Cs^+	0.0	0.0	0.0

[a] The single/double relative free energies are calculated from $[\Delta G^D - \Delta G^S]$, where ΔG^S is the binding free energy of a first ion to an unoccupied channel, and ΔG^D is the binding free energy of a second ion to a singly occupied channel. All free energies are given relative to Cs^+. Details of the MD/FES simulations were given in ref 17.

(f) Channel Gating. Direct observation of the electric current flow through individual ion channels with the patch-clamp method reveals characteristic abrupt transitions between discrete unitary conductance levels. These "gating" transitions correspond to the opening and closing of single ion channel macromolecules. It is believed that the open and closed states of biological channels correspond to different allosteric conformations of the structure (see ref 1). One family of chemical analogues of the GA channel synthesized by Stankovic et al.,[47] in which the two monomers were linked at their N-termini with a dioxolane ring, exhibits a similar phenomenon. The two

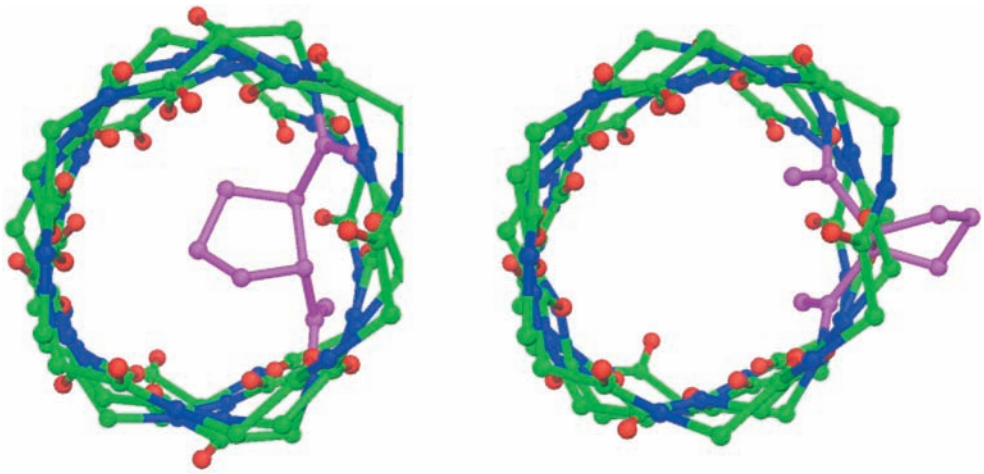

FIGURE 7. View of the *RR*-linked dioxolane GA channel along the pore axis (the side-chain atoms are omitted for the sake of clarity). The closed conformation, with the ring inside the pore (left), and the open conformation, with the ring outside the pore (right), are shown.[24]

stereospecific isomers of the dioxolane-linked GA that were produced, the *SS* and *RR* forms, have strikingly different properties. Frequent and rapid interruptions of a K^+ current ("flickers") were observed in single channel recordings with the *RR*-linked channels, but not with the *SS*-linked channels; the measured blocking rate was 100 s^{-1}, and the average lifetime of blocking was around 0.1 ms. Such flickers, which are not usually observed with channels formed by naturally occurring GA, were interpreted as evidence for conformational transitions of the dioxolane ring from the outside to the inside of the channel, acting as a gate to block the pore. This is illustrated in Figure 7. The two isomers provide a simple molecular model to study gating mechanisms at the microscopic level.

Atomic models of the *RR*- and *SS*-linked GA channels were constructed, and the PMFs along two reaction coordinates were calculated using umbrella sampling.[24] The transition rates were estimated from the PMF in the high friction limit. In the case of the *SS* isomer, the calculated blocking rate and average duration of block are 1×10^{-2} s^{-1} and 0.06 μs, respectively. Such short flickers, which could occur once every 100 s, would not be easily detected under normal experimental conditions. The calculation clearly demonstrated that the *SS* isomer cannot easily flip inside the channel to block the conducting pathway, in qualitative agreement with the experimental results.

In the case of the *RR* isomer, the calculated blocking rate and average duration of block are 280 s^{-1} and 9 ns, respectively. Although the blocking rate has approximately the correct magnitude, the lifetime of the blocked channel is much too short and disagrees sharply with the experimental observations. Since the measurements involved detecting flickers in K^+ current, it might be possible that a K^+ ion in the channel could have a large influence on the lifetime of the blocked channel. To verify this hypothesis, the PMF was recalculated in the case of the *RR* form with a K^+ ion near the center of the dimer channel. The result showed that that the presence of a K^+ ion near the center of the channel stabilizes significantly the dioxolane ring in the blocked channel conformation; the activation energy barrier changes from 5.9 kcal/mol in the water-filled channel to 12.2 kcal/mol when a K^+ ion is present. The calculated lifetime of the blocked state in the presence of a permeating K^+ inside the channel is 0.04 ms, much closer to the experimental value of 0.1 ms.

(g) Proton Wire. Proton transport through GA displays unique properties, implying that the mechanism underlying the conduction of protons is radically different from that of other ions. The diffusion constants inside the pore deduced from experimental ion-flux data indicate that protons move almost 8 times as fast as water molecules themselves.[28] This suggests that the translocation of protons across the GA channel occurs through a succession of hops along the single file of hydrogen-bonded water molecules, which acts effectively as a *proton wire*.[48] It has been demonstrated, by simulating model pores of different width, that mobility of an excess proton is considerably enhanced in the single-file structure relative to bulk water.[49] It is believed that such proton wires play an essential role in several bioenergetic systems.[50]

A model was constructed to study the single file of water molecules of the GA channel and its ability to function as a proton wire.[28] The model included the dimer channel with 22 water molecules and 1 excess proton. The microscopic potential energy surface governing the motion of the water oxygen and hydrogen nuclei was represented with the polarization model (PM6) of Stillinger and co-workers.[51] The basic structural elements of PM6 are H^+ and O^{2-} atoms, which makes it possible to account for the full dissociation of water molecules into ionic fragments. Quantum effects due to the light mass of the hydrogen nuclei were incorporated by exploiting the isomorphism of the discretized Feynman path integral representation of the density matrix with an effective classical system obeying Boltzmann statistics.[27] Following the path integral approach, each proton was replaced in the effective classical system by a ring polymer, or necklace, of $P = 32$ fictitious particles with a harmonic

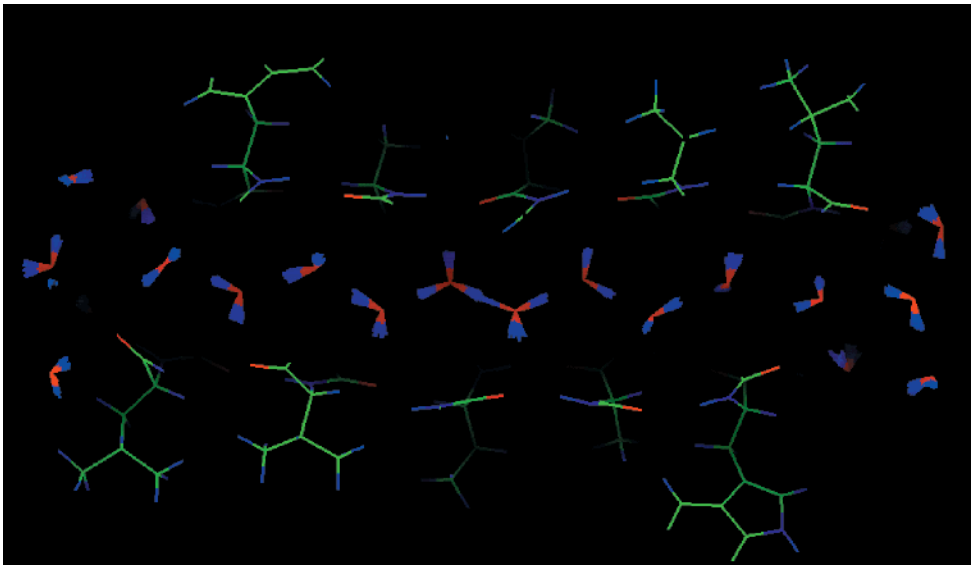

FIGURE 8. Instantaneous configuration of the single-file hydrogen-bonded water chain in the GA channel with one excess proton.[28] On average, each water molecule forms two hydrogen bonds with its neighbors in the single file, and one with a carbonyl oxygen atom on the backbone. The average dispersion of the Feynman path integral ring polymers is about 0.3 Å.

spring between nearest neighbors along the ring. MD simulations of such effective classical system are valid for obtaining ensemble averages, although they do not provide information on the time-dependent quantum dynamics of the system.

The simulation showed that the presence of an excess proton in the pore affects the orientation of the single-file water molecules and water−water hydrogen-bonding interactions. A typical configuration is shown in Figure 8. It is observed that, rather than a well-defined hydronium ion OH_3^+, the protonated species is characterized by a strong hydrogen bond resembling that of $O_2H_5^+$. This was also observed in simulations of simple model systems.[52] The quantum dispersion of protons has a small but significant effect on the equilibrium structure of the hydrogen-bonded water chain.

During classical trajectories ($P = 1$), proton transfer between consecutive water molecules was a very fast spontaneous process, taking place in the subpicosecond time scale. The translocation along extended distances resulted from the interplay of the rapid hydrogen bond length fluctuations. Ultimately, it is the slow reorganization of hydrogen bonds between single-file water molecules and channel backbone carbonyl groups that, by affecting the connectivity and the dynamics of the single-file water chain, also limits the translocation of the proton across the pore.

A kinetic model was formulated to calculate the transport properties of the proton wire and to provide a conceptual framework for incorporating the information extracted from the MD simulations.[53,54] In the kinetic model, the proton wire is represented in terms of two distinct steps involving the propagation of the ionic and hydrogen-bonding defects along the single-file water chain, respectively. The free energy barriers for the propagation of ionic and hydrogen-bonding defects calculated from MD simulations were used as input in the framework model.[55]

IV. Concluding Remarks

Following the rapid evolution in computational methodologies, studies of the GA channel have grown significantly in complexity during the past decade, going from simulations of relatively small systems with a few water molecules[3,21] to sophisticated simulations of large macromolecular assemblies with explicit lipids.[18,35,41,42] It is now almost routinely possible to simulate very realistic atomic models of important biological channels such as OmpF porin from *Escherichia coli* porin,[39,56] the mechanosensitive channel MscL,[57,58] or the KcsA K^+ channel from *Streptomyces lividans*.[59−63]

As shown by the current overview, one can address important questions about ion channels function such as ion binding, ion selectivity, multiple occupancy, and gating using atomistic simulations. However, despite the rapid progress in computational methodologies, MD simulations of ion channels remain very challenging. In this context, it is particularly encouraging to note that several of the early results about the GA channel are entirely consistent with more recent studies. For example, independent simulations at different levels of complexity revealed that the location of the binding sites of Na^+ is near the channel entrance,[21,18] in excellent accord with experimental data.[43−45] This suggests that specific questions can be addressed in a meaningful way on the basis of relatively small calculations and that computationally inexpensive approximations should be expected to play an important role. Continuum electrostatics calculations, in particular, can serve to elucidate fundamental principles about the function of ion channels,[64] though it must be applied to narrow pores with caution.[31] Similarly,

kinetic rate models,[53,54,65] continuum electrodiffusion theory,[66] and stochastic Brownian dynamics (BD)[67−70] represent alternative approaches to calculate ion-flux phenomena at very long time scales. Adopting a hierarchy of approaches might be a powerful computational strategy, though further work will be needed to clarify the inter-relation between the different level of approximations.

References

(1) Hille, B. *Ionic Channels of Excitable Membranes*, 3rd ed.; Sinauer: Sunderland, MA, 2001.
(2) Andersen, O. S.; Koeppe, R. E., II. Molecular determinants of channel function. *Physiol. Rev.* **1992**, *72*, S89−S158.
(3) Roux, B.; Karplus, M. Molecular Dynamics Simulations of the Gramicidin Channel. *Annu. Rev. Biomol. Struct. Dyn.* **1994**, *23*, 731−761.
(4) Arseniev, A. S.; Barsukov, I. L.; Bystrov, V. F.; Lomize, A. L.; Ovchinnikov, Y. A. 1H-NMR study of gramicidin A transmembrane ion channel. Head-to-head, right-handed, single-stranded helices. *FEBS Lett.* **1985**, *186*, 168−174.
(5) Ketchem, R. R.; Hu, W.; Cross, T. A. High-Resolution Conformation of Gramicidin A in Lipid Bilayer by Solid-State NMR. *Science* **1993**, *261*, 1457−1460.
(6) Ketchem, R. R.; Roux, B.; Cross, T. A. High-resolution refinement of a solid-state NMR-derived structure of gramicidin A in a lipid bilayer environment. *Structure* **1997**, *5*, 1655−11669.
(7) Townsley, L. E.; Tucker, W. A.; Sham, S.; Hinton, J. F. Structures of gramicidins A, B, and C incorporated into sodium dodecyl sulfate micelles. *Biochemistry* **2001**, *40*, 11676−11686.
(8) Mackay, D. H.; Berens, P. H.; Wilson, K. R. Structure and dynamics of ion transport through Gramicidin A. *Biophys. J.* **1983**, *46*, 229−248.
(9) McCammon, J. A.; Gelin, B. R.; Karplus, M. Dynamics of folded proteins. *Nature* **1977**, *267*, 585−590.
(10) Džidić, I.; Kebarle, P. Hydration of the Alkali Ions in the gas Phase. Enthalpies and Entropies of Reactions $M^+(H_2O)_{n-1} + H_2O = M^+(H_2O)_n$. *J. Phys. Chem.* **1970**, *74*, 1466−1474.
(11) Klassen, J. S.; Anderson, S. G.; Blades, A. T.; Kebarle, P. Reaction enthalpies for M(+)L = M(+) + L, where M(+) = Na+ and K+ and L equals acetamide, N-methylacetamide, N,N-dimethylacetamide, glycine, and glycylglycine, from determinations of the collision-induced dissociation thresholds. *J. Phys. Chem.* **1996**, *100*, 14218−14227.
(12) Roux, B.; Karplus, M. Potential Energy Function for Cations−Peptides Interactions: An Ab Initio Study. *J. Comput. Chem.* **1995**, *16*, 690−704.
(13) Åqvist, J. Ion water interaction potential derived from free energy perturbation simulations. *J. Phys. Chem.* **1990**, *94*, 8021−8024.
(14) Beglov, D.; Roux, B. Finite representation of an infinite bulk system: Solvent Boundary Potential for Computer Simulations. *J. Chem. Phys.* **1994**, *100*, 9050−9063.
(15) Tissandier, M. D.; Cowen, K. A.; Feng, W. Y.; Gundlach, E.; Cohen, M. H.; Earhart, A. D.; Tuttle, T. R.; Coe, J. V. The proton's absolute aqueous enthalpy and gibbs free energy of solvation from cluster ion solvation data. *J. Phys. Chem. A* **1998**, *102*, 9308−9308.
(16) Roux, B. Nonadditivity in Cation−Peptide Interactions: A Molecular Dynamics and Ab Initio Study of Na^+ in the Gramicidin Channel. *Chem. Phys. Lett.* **1993**, *212*, 231−240.
(17) Roux, B.; Prod'hom, B.; Karplus, M. Ion transport in the gramicidin channel: Molecular dynamics study of single and double occupancy. *Biophys. J.* **1995**, *68*, 876−892.
(18) Woolf, T. B.; Roux, B. The Binding Site of Sodium in the Gramicidin A Channel: A Comparison of Molecular Dynamics Simulations with Solid State NMR Data. *Biophys. J.* **1997**, *72*, 1930−1945.
(19) Zwanzig, R. W. High-temperature equation of state by a perturbation method. *J. Chem. Phys.* **1954**, *22*, 1420−1426.
(20) Torrie, G. M.; Valleau, J. P. Monte Carlo Free Energy Estimates Using Non-Boltzmann Sampling: Application to the Sub-Critical Lennard-Jones Fluid. *Chem. Phys. Lett.* **1974**, *28*, 578−581.
(21) Roux, B.; Karplus, M. Ion Transport in the Gramicidin Channel: Free Energy of the Solvated Right-Handed Dimer in a Model Membrane. *J. Am. Chem. Soc.* **1993**, *115*, 3250−3262.
(22) Chandler, D. Statistical mechanics of isomerization dynamics in liquids and the transition state approximation. *J. Chem. Phys.* **1978**, *68*, 2959−2970.
(23) Berne, B. J.; Borkovec, M.; Straub, J. E. Classical and modern methods in reaction rate theory. *J. Phys. Chem.* **1988**, *92*, 3711−3725.
(24) Crouzy, S.; Woolf, T. B.; Roux, B. A Molecular Dynamics Study of Gating in Dioxolane- Linked Gramicidin A Channels. *Biophys. J.* **1994**, *67*, 1370−1386.
(25) Kollman, P. A. Free Energy Calculations: Applications to Chemical and Biochemical Phenomena. *Chem. Rev.* **1993**, *93*, 2395−2417.
(26) Roux, B. Valence Selectivity of the Gramicidin Channel: A Molecular Dynamics Free Energy Perturbation Study. *Biophys. J.* **1996**, *71*, 3177−3185.
(27) Chandler, D.; Wolynes, P. G. Exploiting the Isomorphism Between Quantum Theory and Classical Statistical Mechanics of Polyatomic Fluids. *J. Chem. Phys.* **1981**, *74*, 4078−4095.
(28) Pomes, R.; Roux, B. Structure and dynamics of a proton wire: a theoretical study of H+ translocation along the single-file water chain in the gramicidin A channel. *Biophys. J.* **1996**, *71*, 19−39.
(29) Roux, B. The influence of the membrane potential on the free energy of an intrinsic protein. *Biophys. J.* **1997**, *73*, 2980−2989.
(30) Roux, B. Statistical mechanical equilibrium theory of selective ion channels. *Biophys. J.* **1999**, *77*, 139−153.
(31) Roux, B.; Bernèche, S.; Im, W. Ion channels, permeation and electrostatics: insight into the function of KcsA. *Biochemistry* **2000**, *39*, 13295−13306.
(32) Brooks, B. R.; Bruccoleri, R. E.; Olafson, B. D.; States, D. J.; Swaminathan, S.; Karplus, M. CHARMM: A program for macromolecular energy minimization and dynamics calculations. *J. Comput. Chem.* **1983**, *4*, 187−217.
(33) Merz K. M., Roux, B., Eds. *Biomolecular Membranes. A molecular perspective from computation and experiment*; Birkhauser: Boston, 1996.
(34) Woolf, T. B.; Roux, B. Molecular dynamics simulation of the gramicidin channel in a phospholipid bilayer. *Proc. Natl. Acad. Sci. U.S.A.* **1994**, *91*, 11631−11635.
(35) Woolf, T. B.; Roux, B. Structure, Energetics and Dynamics of Lipid−Protein Interactions: A Molecular Dynamics Study of the Gramicidin A Channel in a DMPC Bilayer. *Proteins: Struct., Funct. Genet.* **1996**, *24*, 92−114.
(36) Venable, R. M.; Zhang, Y.; Hardy, B. J.; Pastor, R. W. Molecular dynamics simulations of a lipid bilayer and of hexadecane: an investigation of membrane fluidity. *Science* **1993**, *262*, 223−226.
(37) Woolf, T. B.; Malkin, V. G.; Malkin, O. L.; Salahub, D. R.; Roux, B. The Backbone ^{15}N Chemical Shift Tensor of the Gramicidin Channel: A Molecular Dynamics and Density Functional Study. *Chem. Phys. Lett.* **1995**, *239*, 186−194.
(38) Becker, M. D.; Greathouse, D. V.; Koeppe, R. E.; Andersen, O. S. Amino Acid Sequence Modulation of Gramicidin Channel Function: Effetcs of Tryptophane-to-Phenylalanine Substitutions on the Single-Channel Conductance and Duration. *Biochemistry* **1991**, *30*, 8830−8839.
(39) Tieleman, D. P.; Forrest, L. R.; Sansom, M. S.; Berendsen, H. J. Lipid properties and the orientation of aromatic residues in OmpF, influenza M2, and alamethicin systems: molecular dynamics simulations. *Biochemistry* **1998**, *37*, 17554−17561.
(40) Rice D.; Oldfield, E. Deuterium nuclear magnetic resonance studies of the interaction between dimyristoylphosphatidylcholine and gramicidin a. *Biochemistry* **1979**, *18*, 3272−3279.
(41) Chiu, S. W.; Subramaniam, S.; Jakobsson, E. Simulation study of a gramicidin/lipid bilayer system in excess water and lipid. I. Structure of the molecular complex. *Biophys. J.* **1999**, *76*, 1929−1938.
(42) Chiu, S. W.; Subramaniam, S.; Jakobsson, E. Simulation study of a gramicidin/lipid bilayer system in excess water and lipid. II. Rates and mechanisms of water transport. *Biophys. J.* **1999**, *76*, 1939−1950.
(43) Smith, R.; Thomas, D. E.; Atkins, A. R.; Separovic, F.; Cornell, B. A. Solid-state 13c-nmr studies of the effects of sodium ions on the gramicidin a ion channel. *Biochim. Biophys. Acta* **1990**, *1026*, 161−166.
(44) Tian, F.; Lee, K. C.; Hu, W.; Cross, T. A, Monovalent cation transport: lack of structural deformation upon cation binding. *Biochemistry* **1996**, *35*, 11959−11966.
(45) Olah, G. A.; Huang, H. W.; Liu, W.; Wu, Y. The thallium ion distribution in the Gramicidin channel by X-ray diffraction. *J. Mol. Biol.* **1991**, *218*, 847.
(46) Im, W.; Beglov, D.; Roux, B. Continuum solvation model: Electrostatic forces from numerical solutions to the Poisson-Boltzmann equation. *Comput. Phys. Comm.* **1998**, *111*, 59−75.
(47) Stankovic, C. J.; Heinemann, S. H.; Delfino, J. M.; Sigworth, F. J.; Schreiber, S. L. Transmembrane Channels Based on Tartaric Acid−Gramicidin A Hybrid. *Science* **1989**, *244*, 813−817.
(48) Nagle, J. F.; Morowitz, H. J. Molecular Mechanisms for Proton Transport in Membranes. *Proc. Natl. Acad. Sci. U.S.A.* **1978**, *75*, 298−302.
(49) Brewer, M. L.; Schmitt, U. W.; Voth, G. A. The formation and dynamics of proton wires in channel environments. *Biophys. J.* **2001**, *80*, 1691−1702.

(50) Baciou, L.; Michel, H. Interruption of the Water Chain in the Reaction Center from *Rb. sphaeroides* Reduces the Rates of the Proton Uptake and of the Second Electron Transfer to Q_B. *Biochemistry* **1995**, *34*, 7967−7972.
(51) Stillinger, F. H.; David, C. W. Polarization Model for Water and its Ionic Dissociation Products. *J. Chem. Phys.* **1978**, *69*, 1473−1484.
(52) Pomes, R.; Roux, B. Theoretical Study of H+ Translocation along a Model Proton Wire. *J. Phys. Chem.* **1996**, *100*, 2519−2527.
(53) Schumaker, M. F.; Pomes, R.; Roux, B. A combined molecular dynamics and diffusion model of single proton conduction through gramicidin. *Biophys. J.* **2000**, *79*, 2840−2857.
(54) Schumaker, M. F.; Pomes, R.; Roux, B. Framework model for single proton conduction through gramicidin. *Biophys. J.* **2001**, *80*, 12−30.
(55) Pomes, R.; Roux, B. Free energy profiles for H+ conduction along hydrogen-bonded chains of water molecules. *Biophys. J.* **1998**, *75*, 33−40.
(56) Tieleman, D. P.; Berendsen, H. J. C. A Molecular Dynamics Study of the Pores Formed by E. coli OmpF Porin in a Fully Hydrated POPE Bilayer. *Biophys. J.* **1998**, *74*, 2786−2801.
(57) Gullingsrud, J.; Kosztin, D.; Schulten, K. Structural determinants of MscL gating studied by molecular dynamics simulations. *Biophys. J.* **2001**, *80*, 2074−2081.
(58) Elmore, D. E.; Dougherty, D. A. Molecular dynamics simulations of wild-type and mutant forms of the Mycobacterium tuberculosis MscL channel. *Biophys. J.* **2001**, *81*, 1345−1359.
(59) Guidoni, L.; Torre, V.; Carloni, P. Potassium and sodium binding to the outer mouth of the K+ channel. *Biochemistry* **1999**, *38*, 8599−8604.
(60) Shrivastava, I. H.; Sansom, M. S. Simulations of ion permeation through a potassium channel: molecular dynamics of KcsA in a phospholipid bilayer. *Biophys. J.* **2000**, *78*, 557−570.
(61) Bernèche, S.; Roux, B. Molecular dynamics of the KcsA K(+) channel in a bilayer membrane. *Biophys. J.* **2000**, *78*, 2900−2917.
(62) Crouzy, S.; Bernèche, S.; Roux, B. Extracellular Blockade of K^+ Channels by TEA: Results from Molecular Dynamics Simulations of the KcsA channel. *J. Gen. Physiol.* **2001**, *118*, 207−217.
(63) Bernèche, S.; Roux, B. Energetics of ion conduction through the k+ channel. *Nature* **2001**, *414*, 73−77.
(64) Roux, B.; MacKinnon, R. The cavity and pore helices in the KcsA K+ channel: electrostatic stabilization of monovalent cations. *Science* **1999**, *285*, 100−102.
(65) McGill, P.; Schumaker, M. F. Boundary conditions for single-ion diffusion. *Biophys. J.* **1996**, *71*, 1723−1742.
(66) Kurnikova, M. G.; Coalson, R. D.; Graf, P.; Nitzan, A. A lattice relaxation algorithm for three-dimensional Poisson−Nernst−Planck theory with application to ion transport through the gramicidin A channel. *Biophys. J.* **1999**, *76*, 642−656.
(67) Jakobsson, E.; Chiu, S. W. Stochastic theory of ion movement in channels with single-ion occupancy. Application to sodium permeation of gramicidin channels. *Biophys. J.* **1987**, *52*, 33−45.
(68) Chung, S. H.; Allen, T.; Hoyles, M.; Kuyucak, S. Permeation of ions across the potassium channel: brownian dynamics studies. *Biophys. J.* **1999**, *77*, 2517−2533.
(69) Im, W.; Seefeld, S.; Roux, B. A. Grand Canonical Monte Carlo−Brownian Dynamics Algorithm for Simulating Ion Channels. *Biophys. J.* **2000**, *79*, 788−801.
(70) Im, W.; Roux, B. Brownian Dynamics Solutions of Ions Channels: A General Treatment of Electrostatic Reaction Fields for Molecular Pores of Arbitrary Geometry. *J. Chem. Phys.* **2001**, *115*, 4850−4861.

AR010028V